

# A note on the use of intensity vector maps for source identification

Daniel Juvé

Laboratoire de Mécanique des Fluides et d'Acoustique, UA CNRS 263, Ecole Centrale de Lyon, B.P. 163-69131 Ecully Cedex, France

(Received 2 November 1987; accepted for publication 18 January 1988)

A procedure to identify noise sources from intensity vector maps is presented. It is based on the minimization, in a mean-squares sense, of the difference between the measured intensity field and an estimated one. The sensitivity of this inversion scheme to small random errors in the data is then studied by numerical simulations. It is shown that good estimates of the positions and strengths of the noise sources are obtained only when the measurements are made in the close vicinity of the source region.

PACS numbers: 43.85.Fm, 43.28.Tc, 43.88.Kb, 43.50.Yw

## INTRODUCTION

In recent years, the two-microphone method of measuring acoustic intensity<sup>1,2</sup> has received increasing attention and has become a powerful tool for studying a variety of acoustic phenomena. Moreover, different types of probes have been developed to determine two or three components of the *intensity vector*.<sup>3,4</sup> Detailed maps of these vectors have been obtained in the nearfield of complicated sources, vibrating bodies,<sup>3</sup> and jets,<sup>5</sup> leading to a qualitative identification of strong radiating regions and of preferred paths for energy flow.

However, little work has been done to evaluate the potential of intensity vector maps in obtaining precise values of the positions and strengths of noise sources. An inversion scheme has been suggested by the author<sup>6</sup> and applied to locate the center of mass of the continuous source distribution in clean or excited turbulent air jets.<sup>7</sup> It is based on the minimization of the difference, in a mean-squares sense, between a measured intensity field and an estimated one. Recently, some variants of this technique have been used for numerical simulations in noise-free conditions.<sup>8,9</sup>

In this article, a simple radiation model is used to study the influence of small random errors in the data on the accuracy of the identification procedure. Numerical simulations demonstrated that the measurements have to be made in the close vicinity of the sources in order to obtain good results. As a simple rule, the points of observation have to be placed at a distance from the source region shorter than the separation between two neighboring sources.

## I. FORMULATION OF THE DIRECT PROBLEM

To test the inversion scheme, a very simple radiation model has been chosen. The sources are statistically independent monochromatic point monopoles. They are located at constant intervals along a straight line (Fig. 1). The points of observation are placed on a parallel line, a distance  $Y$  apart, so that the problem is two dimensional.

The components  $I_{x_j}$  and  $I_{y_j}$  of the intensity vector at point  $j$  are readily calculated:

$$I_{x_j} = \frac{1}{\rho c} \sum_{i=1}^{NS} \frac{p_i^2}{r_{ij}^2} \cos \theta_{ij},$$

$$I_{y_j} = \frac{1}{\rho c} \sum_{i=1}^{NS} \frac{p_i^2}{r_{ij}^2} \sin \theta_{ij},$$
(1)

where  $\theta_{ij}$  and  $r_{ij}$  define the relative positions of the  $i$ th source and of the  $j$ th point of observation, and  $p_i$  is the monopole amplitude of source  $i$ .

These formulas can be written in a matrix form, convenient for latter use:

$$\mathbf{I} = \mathbf{H}\mathbf{S},$$
(2)

where  $\mathbf{I}$  is a column vector of dimensions  $(2NP, 1)$ ,  $\mathbf{I}^T = (I_{x_1}, I_{y_1}, I_{x_2}, I_{y_2}, \dots)$ ;  $\mathbf{S}$  a column vector of dimensions  $(NS, 1)$ ,  $\mathbf{S}^T = (p_1^2, p_2^2, \dots)$ ; and  $\mathbf{H}$  a matrix of dimensions  $(2NP, NS)$  characterizing the geometry of the problem (observation matrix).

When the positions  $X_s$  and strengths  $p_i^2$  are known, the intensity field is easily computed. The problem of interest for us is the following: If the intensity vectors are given, perhaps with small random uncertainties simulating the measurement errors, is it possible to obtain good estimates of the positions and levels of the sources?

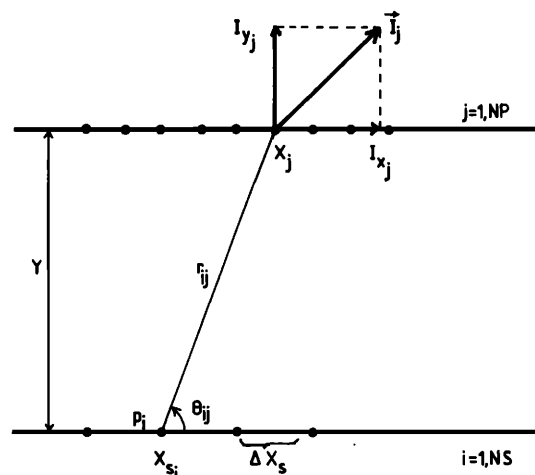


FIG. 1. Definition of the geometric parameters for the radiation model.

## II. FORMULATION OF THE INVERSE PROBLEM

The natural approach to solve this inverse problem is to search for the unknowns  $(X_{S_i}, p_i^2)$  by minimizing, in a mean-squares sense, the difference between the given intensity field and the one calculated from estimates of the positions and the levels with the help of Eq. (1).

When the positions of the sources are known, the problem is linear in the  $p_i^2$ , so that the least-squares estimator  $\hat{S}_{LS}$  of the true source vector  $S$  is given by the pseudoinverse (or generalized inverse) of  $H$ :

$$\hat{S}_{LS} = (H^T H)^{-1} H^T \mathbf{I}. \quad (3)$$

The difference between the observed values and those predicted is named the residual  $\mathbf{r}$ :

$$\mathbf{r} = \mathbf{I} - \hat{\mathbf{I}}_{LS}, \quad \hat{\mathbf{I}}_{LS} = H \hat{S}_{LS}. \quad (4)$$

When both the positions and the amplitudes of the sources are unknown, the following procedure is applied.

(a) A starting point  $\{X_{S_i}^0\}$  is chosen, (b) a first estimate of  $S$  is computed from Eq. (3) and the residual  $\mathbf{r}$  is evaluated, and (c) the source position vector  $\{X_{S_i}\}$  is changed using an optimization algorithm to minimize the "cost function"  $F = \|\mathbf{r}\|^2 / \|\mathbf{I}\|^2$ .

In practice, the direct research (that is gradient-free) procedure of Powell<sup>10</sup> has been used. Since the estimates of the  $p_i^2$  may be negative, positivity constraints have been added by artificially increasing the cost function  $F$  when this is the case (penalty method). *A priori* information on the approximate positions of the sources can be introduced in the same manner. No effort has been made to choose the most efficient optimization algorithm, but the selected procedure works very well and converges rapidly when the number of sources is not too high ( $NS < 10$ ). Typical results are given below, first for the noise-free case and then with simulated measurement errors.

## III. RESULTS

### A. Noise-free case

In this perfect case, only numerical round-off errors are present and, as expected, very good results are obtained from the inversion procedure. Typical examples are given in Table I in the case of three sources observed at a reduced distance  $Y^* = Y/\Delta X_S = 3$ .

### B. Simulation of measurement errors

To simulate the statistical errors inherent in any measurement, the components of the intensity vectors [initially calculated from Eq. (1)] have been multiplied by a sequence of (pseudo) random numbers. These numbers had a Gaussian distribution with a zero mean and a relative standard deviation  $\sigma = 0.025$  or  $0.05$ . Some typical results are given in Table II, in the case of two sources of equal magnitude, observed at various reduced distances  $Y^*$ .

It is clear from this table that good estimates are obtained for the smaller observation distance ( $Y^* = 1$ ) but that considerable scatter occurs for  $Y^* = 2$  and  $3$ . To quantify this scatter in one number, we have defined a composite relative error as

TABLE I. Identification of sources in the noise-free case—21 points of observation at positions ranging from  $-5\Delta X_S$  to  $5\Delta X_S$ . Starting point:  $X_{S_1}^0 = -1.2$ ,  $X_{S_2}^0 = 0.2$ ,  $X_{S_3}^0 = 1.3$ .

	$X_{S_1}$	$p_1^2$	$X_{S_2}$	$p_2^2$	$X_{S_3}$	$p_3^2$
True values	-1	1	0	1	1	1
	$\hat{X}_{S_1}$	$\hat{p}_1^2$	$\hat{X}_{S_2}$	$\hat{p}_2^2$	$\hat{X}_{S_3}$	$\hat{p}_3^2$
Estimates	-1	0.997	$10^{-3}$	1	0.998	1
	$X_{S_1}$	$p_1^2$	$X_{S_2}$	$p_2^2$	$X_{S_3}$	$p_3^2$
True values	-1	1	0	5	1	1
	$\hat{X}_{S_1}$	$\hat{p}_1^2$	$\hat{X}_{S_2}$	$\hat{p}_2^2$	$\hat{X}_{S_3}$	$\hat{p}_3^2$
Estimates	-0.999	1	$6 \times 10^{-4}$	5	1	0.997

$$e = \sum_{i=1}^{NS} \frac{\|X_{S_i} - \hat{X}_{S_i}\|^2}{\|X_{S_i}\|^2} + \sum_{i=1}^{NS} \frac{|p_i^2 - \hat{p}_i^2|}{p_i^2}, \quad (5)$$

with the results

$$e(Y^* = 1) = 0.04, \quad e(Y^* = 2) = 0.57, \quad (6)$$

$$e(Y^* = 3) = 0.64.$$

In each case the intensity vector field is estimated with excellent precision; the relative error ranges from 0.017 to 0.025, which corresponds closely to the standard deviation of the simulated random errors.

The influence of the number of measurement points on the cumulative error is shown in Fig. 2 for four values of  $Y^*$ . As expected, increasing the amount of data produces a decrease of the estimation error, but rapidly the latter becomes stabilized and no further dramatic benefit is obtained in our configurations for  $NP > 21$ . It then appears that the problem of the identification of sources from intensity vectors is, in certain circumstances, "ill-posed,"<sup>11</sup> that is, the results of the inversion may be too sensitive to small variations in the data to be of any practical interest. The essential parameter that controls this ill-posedness is the distance  $Y$  between the line of observation and the line of the sources. Other parameters, such as the separation between measurement points, the angular cover of the source field, etc., play only minor roles.

TABLE II. Identification of sources in the presence of simulated measurement errors ( $\sigma = 0.025$ ). Twenty-one points of observation at positions ranging from  $-5\Delta X_S$  to  $5\Delta X_S$ .

	$X_{S_1}$	$p_1^2$	$X_{S_2}$	$p_2^2$
True values	-0.5	1	0.5	1
	$\hat{X}_{S_1}$	$\hat{p}_1^2$	$\hat{X}_{S_2}$	$\hat{p}_2^2$
Estimates	$Y^* = 1$	-0.518	0.985	0.493
	$Y^* = 2$	-0.448	1.15	0.619
	$Y^* = 3$	-0.44	1.21	0.68

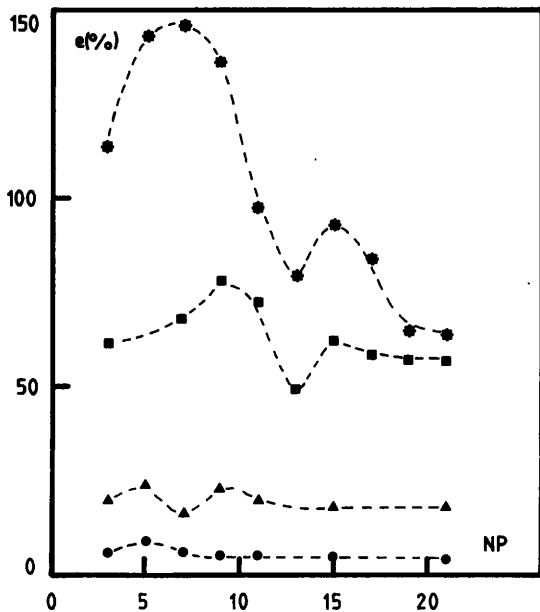


FIG. 2. Evolution with the number of measurement points of the error on the identification of two sources (●,  $Y^* = 1$ ; ▲,  $Y^* = 1.5$ ; ■,  $Y^* = 2$ ; \*,  $Y^* = 3$ ).

Looking at the cost function in a simple case offers another point of view on the ill-posedness of the inversion procedure. We have considered two sources of equal strength ( $p_1^2 = p_2^2 = 1$ ) placed at  $X_{S_1} = -0.5$  and  $X_{S_2} = 0.5$ . The intensity field was computed at  $Y^* = 1$  and  $Y^* = 3$ . Then the sources were moved from 0 to  $-1$  and 0 to 1, respectively, and for each couple  $(X_{S_1}, X_{S_2})$  the least-squares estimate and the cost function  $F$  were formed. The resulting 3-D plots of  $F$  as a function of  $(X_{S_1}, X_{S_2})$  are given in Figs. 3–6 with and without added noise (to enhance the contrast, the quantity really plotted is  $-\log F$ ). Figure 3 corresponds to  $Y^* = 1$  in the noise-free case; a clear optimum for  $F$  is present for  $X_{S_1} = 0.5$ ;  $X_{S_2} = 0.5$ , the value of  $F$  being only limited by round-off errors ( $F_{\text{opt}} \sim 10^{-7}$ ). For  $Y^* = 3$ , the behavior of  $F$  is similar but there is also a line along which  $F$  is very small ( $F \sim 5 \times 10^{-3}$ ), even for source positions far from the exact ones. With noise added on the data at  $Y^* = 1$ , the narrow

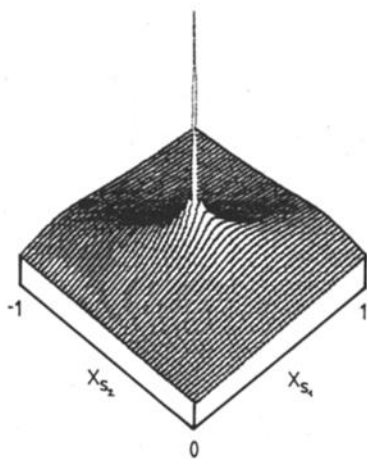


FIG. 3. Plot of the cost function ( $-\log F$ ) in the noise-free case (reduced distance of observation  $Y^* = 1$ ).

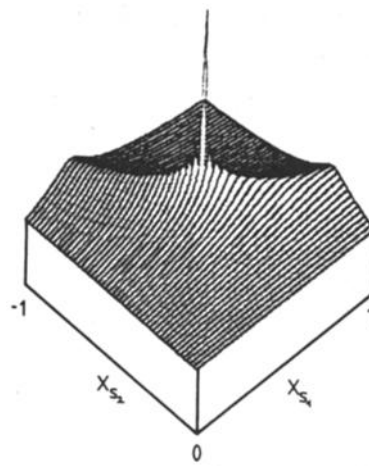


FIG. 4. Plot of  $-\log F$  in the noise-free case ( $Y^* = 3$ ).

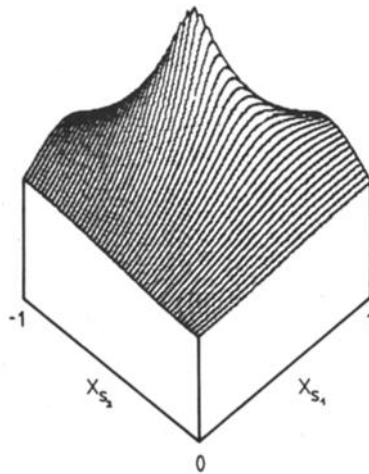


FIG. 5. Plot of  $-\log F$  when measurement errors are simulated (standard deviation  $\sigma = 0.025$ ;  $Y^* = 1$ ).

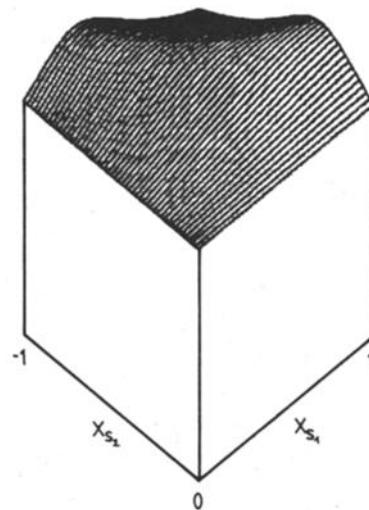


FIG. 6. Plot of  $-\log F$  when measurement errors are simulated ( $\sigma = 0.025$ ;  $Y^* = 3$ ).

peak has turned into a broad hump centered on the true values (Fig. 5) so that it is clear that the identification procedure will give good results in this case. For  $Y^* = 3$ , on the other hand (Fig. 6), the peak has disappeared and only a ridge persists along which the value of  $F$  is more or less constant ( $F \sim 2-3 \times 10^{-2}$ ). In that case the inversion of the intensity vector map will give meaningless estimates of the positions and strengths of the sources. This ambiguity in the identification of noise sources is a consequence of the well-known result that different source distributions can have very similar radiation fields. This is true even when the type of source is prescribed (independent point monopoles in our model), at the exception of the very nearfield. It is to be noted that in our numerical experiments no problem of non-uniqueness appeared: The inversion algorithm converged to the same result (to a given accuracy) for different starting points.

#### IV. CONCLUSION

The use of an optimization procedure to identify acoustic sources from intensity vector maps has been studied by numerical simulation. It has been shown that the inversion procedure works very well in ideal cases but that in certain circumstances it is highly sensitive to small random fluctuations in the data, simulating measurement errors. This imposes severe limitations on the distance separating the measurement probes from the source region. As a simple rule, this distance must be shorter than the separation between two neighboring sources. In our view this does not preclude the application of the inversion method to practical cases, since intensity is essentially a nearfield technique. However, further studies are needed (numerical simulations and/or experiments) to observe the sensitivity of the technique to

errors in the radiation model (such as small departures from omnidirectionality), to partial correlation between the sources, etc. A comparison of the optimization approach with a back propagation algorithm<sup>12</sup> would also be interesting in a case where the acoustic wavelength is longer than the spacing between the sources.

<sup>1</sup>F. J. Fahy, "Measurement of acoustic intensity using the cross-spectral density of two microphone signals," *J. Acoust. Soc. Am.* **62**, 1057-1059 (1977).

<sup>2</sup>G. Pavic, "Measurement of sound intensity," *J. Sound Vib.* **51**, 533-545 (1977).

<sup>3</sup>O. K. Pettersen and U. R. Kristiansen, "Describing acoustic energy flow in two dimensions by the use of intensity vectors," in *Recent Developments in Acoustic Intensity Measurement* (Cetim, Senlis, France, 1981), pp. 103-109.

<sup>4</sup>P. Sas and R. Snoeys, "Visualization and estimation of the near field acoustic intensity," in *Recent Developments in Acoustic Intensity Measurement* (Cetim, Senlis, France, 1981), pp. 119-126.

<sup>5</sup>D. Juvé and P. Roland, "Intensimétrie à deux dimensions—Mesures dans le champ proche d'un jet," *Rev. Acoust.* **66**, 170-176 (1983).

<sup>6</sup>D. Juvé, "Identification de sources ponctuelles à partir de mesures du vecteur intensité acoustique," 11th ICA, Paris (1983), Vol. 1, pp. 279-282.

<sup>7</sup>D. Juvé, "Aeroacoustique des jets excités," D. es Sc. thesis, No. 85.21, Université Lyon I, Lyon, France (1985).

<sup>8</sup>M. Sidki, C. Legros, J. P. Guilhot, and J. P. Flenner, "Caractérisation et localisation des sources acoustiques par des méthodes d'optimisation," *2nd International Congress on Acoustic Intensity* (Cetim, Senlis, France, 1985), pp. 433-440.

<sup>9</sup>C. Legros, M. Sidki, and J. P. Guilhot, "Caractérisation et localisation des sources acoustiques par des méthodes d'optimisation," Paper C8-6, 12th ICA, Toronto, Canada (1986).

<sup>10</sup>H. W. Sorenson, *Parameter Estimation—Principles and Problems* (Dekker, New York, 1980).

<sup>11</sup>A. N. Tikhonov and V. Y. Arsenin, *Solutions of Ill-posed Problems* (Halsted, Washington, DC, 1977).

<sup>12</sup>E. G. Williams, J. D. Maynard, and E. Skudrzyk, "Sound source reconstruction using a microphone array," *J. Acoust. Soc. Am.* **68**, 340-344 (1980).